symmetry

MDPI

Article

Design, Synthesis, and In Vitro Antiproliferative Screening of New Hydrazone Derivatives Containing *cis*-(4-Chlorostyryl) Amide Moiety

Tarfah Al-Warhi [1], Leena S. Alqahtani [2], Matokah Abualnaja [3], Saba Beigh [4], Ola A. Abu Ali [5], Fahmy G. Elsaid [6,7], Ali A. Shati [6], Rasha Mohammed Saleem [8], Ali Hassan Ahmed Maghrabi [9], Amani Abdulrahman Alharthi [10], Amal Alyamani [10], Eman Fayad [10], Ali H. Abu Almaaty [11], Islam Zaki [12,*] and Shaimaa Hamouda [7]

[1]   Department of Chemistry, College of Science, Princess Nourah Bint Abdulrahman University, P.O. Box 84428, Riyadh 11671, Saudi Arabia
[2]   Department of Biochemistry, College of Science, University of Jeddah, Jeddah 23445, Saudi Arabia
[3]   Department of Chemistry, Faculty of Applied Science, Umm Al-Qura University, Makkah Al Mukarramah 24381, Saudi Arabia
[4]   Department of Public Health, Faculty of Applied Medical Sciences, Albaha University, Albaha 65431, Saudi Arabia
[5]   Department of Chemistry, College of Science, Taif University, P.O. Box 11099, Taif 21944, Saudi Arabia
[6]   Biology Department, Science College, King Khalid University, Abha 61421, Saudi Arabia
[7]   Zoology Department, Faculty of Science, Mansoura University, P.O. Box 70, Mansoura 35516, Egypt
[8]   Department of Laboratory Medicine, Faculty of Applied Medical Sciences, Albaha University, Albaha 65431, Saudi Arabia
[9]   Department of Biology, Faculty of Applied Science, Umm Al-Qura University, Makkah 24381, Saudi Arabia
[10] Department of Biotechnology, College of Sciences, Taif University, P.O. Box 11099, Taif 21944, Saudi Arabia
[11] Zoology Department, Faculty of Science, Port Said University, Port Said 42526, Egypt
[12] Pharmaceutical Organic Chemistry Department, Faculty of Pharmacy, Port Said University, Port Said 42526, Egypt
*   Correspondence: eslam.zaki@pharm.psu.edu.eg

Abstract: Hydrazones are regarded as a distinctive category of organic compounds because of their tremendous characteristics and potential uses in analytical, chemical, and medicinal chemistry. In the present study, a new series of Hydrazone Derivatives bearing *cis*-(4-chlorostyryl) amide moiety were designed and synthesized. In vitro cytotoxicity screening showed that compounds **3i, 3l, 3m,** and **3n** revealed potent anticancer activity against MCF-7 cancer cell line with IC_{50} values between 2.19–4.37 μM compared with Staurosporin as a reference compound. The antiproliferative activity of these compounds appears to be correlated well with their ability to inhibit the VEGFR-2 kinase enzyme. Activation of the damage response pathway leads to cellular cycle arrest at the G1 phase. Fluorochrome Annexin V/PI staining indicated that cell death proceeds through the apoptotic pathway mechanism. The mechanistic pathway was confirmed by a significant increase in the level of active *c*aspase 9 compared with control untreated MCF-7 cells.

Keywords: hydrazone derivatives; *cis*-4-chlorostyryl amide; synthesis; cytotoxicity; VEGFR-2; cell cycle analysis; annexin V; *c*aspase

1. Introduction

Cancer has remained one of the most difficult and potentially fatal illnesses to cure [1]. Cancer has been revealed to remain the second largest source of demise worldwide after cardiovascular disorders (CVD) [2,3]. Reported studies confirm that so far, around 22.5 million people have received a cancer diagnosis [4]. Additionally, resistance to the present treatment and adverse effects linked to conventional non-selective chemotherapeutic treatments promote the development of innovative anticancer medicines [5,6]. The protein tyrosine kinases can regulate the cell cycle progression, migration, survival,

differentiation, and proliferation [7]. Tyrosine kinases are able to phosphorylate tyrosine residues in proteins [8]. The function of the proteins is changed as a result of phosphorylation [9]. Tyrosine kinases become continuously active as a result of mutations and/or dysregulation, which eventually lead to the development of cancer [10,11]. Part of the tyrosine kinase is the vascular endothelium growth factor receptor (VEGFR-2) kinase which is recognized to be the primary signal transducer of VEGF-dependent angiogenesis [12]. The accessibility, survivability, and proliferation of the vascular endothelial cells are regulated via the VEGFR-2 signaling pathway [13]. VEGFR-2 is upregulated in a plethora of cancers, which include breast cancer [14]. This is desirable because VEGFR-2 is only tenuously expressed in healthy tissue [15]. As a result, it is thought that blocking the VEGF/VEGFR signaling pathway may be an effective therapeutic target for preventing tumorigenesis besides consequent cancer development [16].

Hydrazones represent an important motif for many bioactive molecules and drugs that possesses a wide range of pharmacological activities [17,18]. A lot of research has been done on hydrazone function because of their many different characteristics and potential uses in analytical, chemical, and medicinal chemistry [19–22]. Hydrazones are regarded as a distinctive category of organic compounds. They played an important role as a building unit for several anticancer agents due to the presence of hydrogen bond donors and acceptors in addition to their flexible skeleton [23,24]. (S)-Naproxen hydrazone molecule **I** showed potent anticancer activity against two different human cancer cell lines (MDA-MB-231 and MCF-7) with good selectivity (IC$_{50}$ = 22.42 and 59.81 μM, respectively) [25]. In addition, SAR studies prove that the antiproliferative activity of PAC-1, **II** is dependent on the presence of hydrazone moiety, which can chelate zinc that allows procaspases 3 to process itself to active form [26]. Furthermore, hydrazone-based aryl sulphonate molecule **III** induced apoptosis in MCF-7 cells at its IC$_{50}$ dose value (IC$_{50}$ = 17.8 μM) mediated through the intrinsic apoptotic pathway by activating *c*aspase 3 and *c*aspase 9 [27]. Further, the cytotoxic effect of hydrazone molecule **IV** was associated with VEGFR-2 inhibition with an IC$_{50}$ value of 0.05 μM as compared with Sorafenib (IC$_{50}$ = 0.10 μM) as a reference drug [28] (Figure 1).
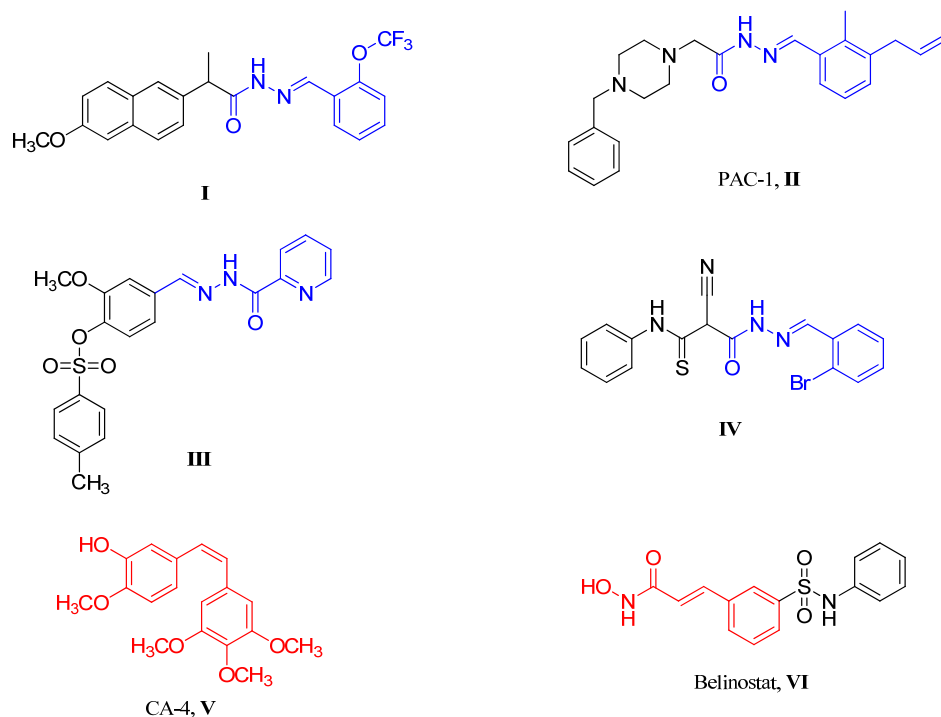

Figure 1. Chemical structures of some reported hydrazone linkage-based anticancer agents (**I**–**IV**) and some potent styryl-containing compounds as anticancer drugs (**V**,**VI**).

The styryl functionality is widely represented in pharmaceutically active molecules, including bioactive molecules and drugs [29–31]. The *cis* combretastatin A-4 (CA-4) **V**, a *cis*-stilbenoid natural product, displayed potent anticancer activity over various cancer cells [32]. In addition, Belinostat **VI** is an FDA-approved styryl hydroxamide molecule that is used to treat cancer [33] (Figure 1).

In this context, our goal was to create a brand-new collection of hydrazone derivatives with a *cis*-(4-chlorostyryl) amide moiety (Figure 2). In an effort to find prospective anticancer agents, the generated hydrazone compounds were evaluated for their in vitro cytotoxic activity against the MCF-7 cancer cell line in comparison with Staurosporin (STU), which served as the reference anticancer molecule. To examine the molecular pathways of the antiproliferative activity of the synthesized hydrazone compounds, additional studies such as the VEGFR-2 inhibitory activity, cell cycle analysis, and apoptosis-related tests were carried out on the most powerful cytotoxic compounds.
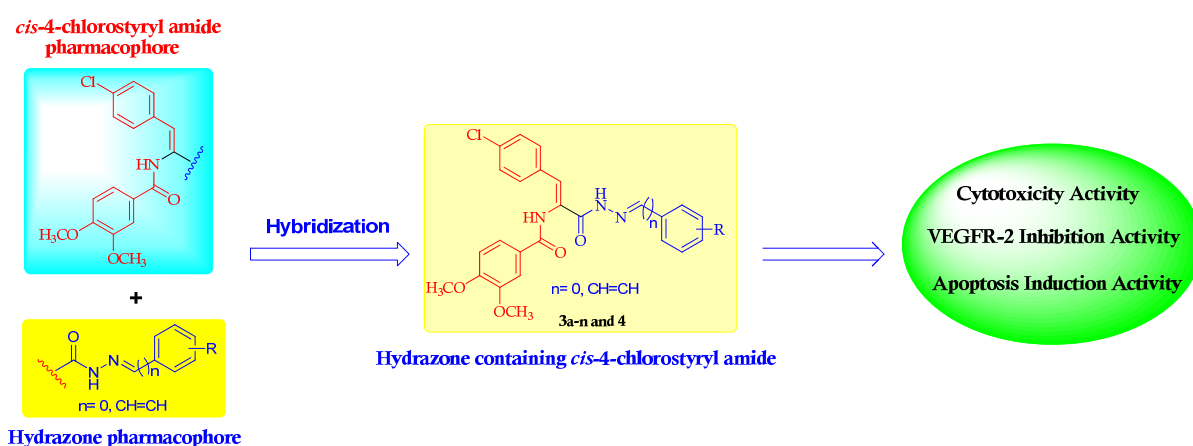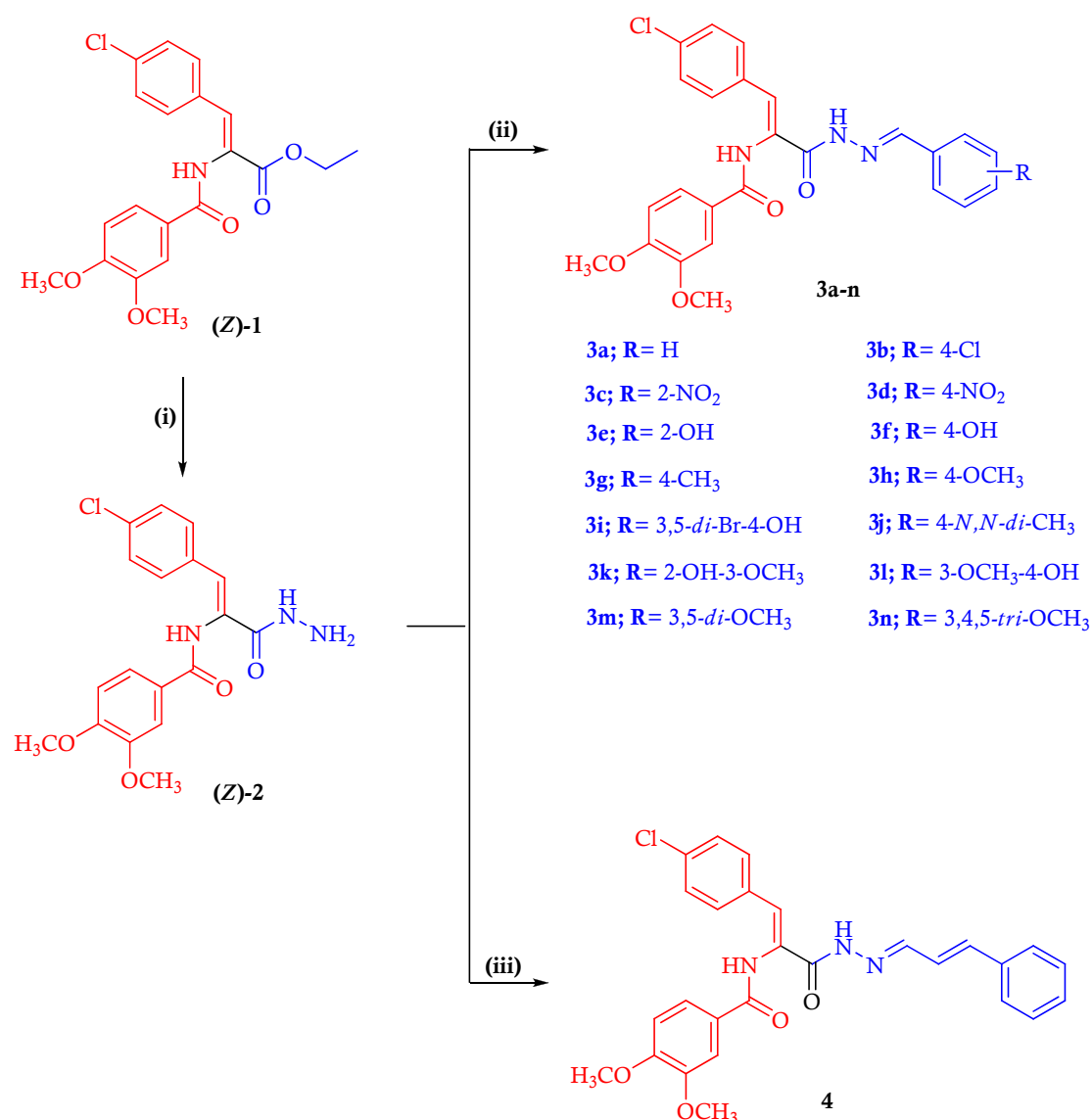

Figure 2. Design strategy of the target hydrazone derivatives containing *cis*-(4-chlorostyryl) amide moiety **3a–n** and **4**.

2. Results and Discussion

2.1. Chemistry

The designed hydrazone-based compounds were synthesized as outlined in Scheme 1. (*Z*)-*N*-(1-(4-chlorophenyl)-3-hydrazinyl-3-oxoprop-1-en-2-yl)-3,4-dimethoxybenzamide (**2**) the key intermediate for the synthesis of the title hydrazone molecules **3a–n** and **4** was prepared by hydrazinolysis of (*Z*)-ethyl 3-(4-chlorophenyl)-2-(3,4-dimethoxybenzamido)acrylate (**1**) in pure ethanol as reported earlier [34]. Treatment of the acid hydrazide (*Z*)-**2** with a respective aromatic aldehyde in pure ethanol containing a few drops of glacial acetic acid afforded the desired hydrazone derivatives **3a–n**. All structures of novel hydrazone derivatives were substantiated by ^{1}H-NMR and ^{13}C-NMR spectra, along with elemental microanalyses data. The ^{1}H-NMR spectrum of 4-methylbenzylidene hydrazinyl derivative **3g**, as a representative example, displayed signals at δ 11.68 and 9.99 ppm assigned to two NH protons, in addition to singlet signal at δ 8.38 ppm due to proton attached to imine (CH=N) carbon. A *Z*-configuration of the olefinic (C=C) bond in the 4-chlorostyryl moiety was confirmed by the signal of olefinic (CH=) proton, which resonated at higher chemical shift at δ 7.06 ppm as a singlet signal. Further, compound **3g** showed the presence of extra signals related to 4-methylphenyl protons together with other signals assigned to 4-chlorostyryl and 3,4-dimethoxyphenyl moieties. The ^{13}C-NMR spectrum of 4-methylbenzylidene hydrazinyl derivative **3g** was compatible with the proposed structure. Thus, in the ^{13}C-NMR spectrum of 4-methylbenzylidene hydrazinyl **3g**, two characteristic signals at δ 165.85 and 162.66 ppm related to hydrazinyl and aromatic amide carbonyl carbons, respectively. Further, the ^{13}C-NMR spectrum of methylbenzylidene hydrazinyl **3g** displayed a signal at δ 147.86 ppm assigned to azomethine (C=N) carbon and signals related to two methoxy (2OCH$_3$) and methyl (CH$_3$) groups at δ 56.17, 56.08 and 21.50 ppm, subsequently. Addition-

ally, the ^{13}C-NMR spectrum of 4-methylbenzylidene hydrazinyl **3g** elicited extra aromatic carbon signals of the introduced 4-methylphenyl moiety that appeared in the region of δ 152.33–111.45 ppm. 3-Phenylallylidene hydrazinyl molecule **4** was obtained by reacting the key acid hydrazide intermediate (**Z**)-**2** with cinnamaldehyde in glacial acetic acid. Thus, in the ^{1}H-NMR spectrum of 3-phenylallylidene hydrazinyl **4**, NH protons appear as two singlet signals at δ 11.65 and 9.97 ppm, respectively as well as characteristic doublet signal at δ 8.20 ppm assignable to azomethine (-N=CH-) proton. Further, 3-phenylallylidene hydrazinyl **4** indicated the presence of two triplet and doublet signals at δ 7.34 and 7.10 ppm, respectively, assigned to two allylic protons of phenylallylidene moiety. In addition, the ^{1}H-NMR spectrum of 3-phenylallylidene hydrazinyl **4** displayed extra aromatic signals in the region of δ 7.74–7.40 ppm corresponding to phenyl protons of the phenylallylidene moiety. The ^{13}C-NMR spectrum of 3-phenylallylidene hydrazinyl **4** revealed the presence of signals for hydrazinyl and amide carbonyl (C=O) at δ 165.83 and 162.60 ppm, in addition to two methoxy carbons at δ 56.17 and 56.09 ppm. Further, 3-phenylallylidene hydrazinyl **4** showed additional carbon signals in the region of δ 152.34–111.45 ppm due to the carbons of the 4-phenylallylidene moiety.

3a; R= H   **3b; R= 4-Cl**

3c; R= 2-NO$_2$ **3d; R= 4-NO$_2$**

3e; R= 2-OH   **3f; R= 4-OH**

3g; R= 4-CH$_3$ **3h; R= 4-OCH$_3$**

3i; R= 3,5-*di*-Br-4-OH   **3j; R= 4-*N,N-di*-CH$_3$**

3k; R= 2-OH-3-OCH$_3$ **3l; R= 3-OCH$_3$-4-OH**

3m; R= 3,5-*di*-OCH$_3$ **3n; R= 3,4,5-*tri*-OCH$_3$**

Scheme 1. Synthesis of the target hydrazone compounds **3a–n** and **4**. Reagents and reaction condition: (i) Hydrazine hydrate, ethanol, reflux 2 h, 84%; (ii) appropriate aromatic aldehyde, ethanol, reflux 5–6 h, 58–79%; (iii) cinnamaldehyde, glacial acetic acid, reflux 4 h, 82%.

2.2. Biology

2.2.1. In Vitro Cytotoxic Activity against MCF-7 Breast Cancer Cell Line

To assess the cytotoxic activity of the prepared hydrazone derivatives **3a–n** and **4**, the breast adenocarcinoma (MCF-7) cell line was involved in the cytotoxicity study, and MTT stain was used to assess cell viability. Staurosporin (STU) was included as a reference anticancer compound in the current study. STU displayed an IC_{50} value of 4.19 μM against MCF-7. The in vitro cytotoxicity results showed that all hydrazone derivatives displayed cytotoxic activity against the MCF-7 cell line with varying IC_{50} values of 2.19–86.44 μM. The most potent aryl hydrazinyl compounds were **3i**, **3l**, **3m,** and **3n** and exhibited IC_{50} values of 4.37, 2.19, 2.88, and 3.51 μM, subsequently (Table 1). All other derivatives were less cytotoxic, with IC_{50} values from 6.19–86.44 μM. Interestingly, 4-hydroxy-3-methoxybenzylidene hydrazinyl molecule **3l** possessed the highest promising cytotoxic effect as concluded from its IC_{50} value (IC_{50} value of 2.19 μM) against test MCF-7 cells compared with the value of 4.19 μM for STU. It could be concluded that substitution on the phenyl ring of arylidene hydrazinyl moiety with electron-donating groups contributed to the cytotoxic activity. Further, the replacement of phenyl ethylidene moiety with phenyl allylidene moiety leads to a reduction of the cytotoxic activity against the MCF-7 cell line.

Table 1. Cytotoxic screening of the tested hydrazone molecules **3a–n** and **4** against MCF-7 breast cancer cell line. Data expressed as mean ± SD.

Comp. No.	IC_{50} Value (μM)
	MCF-7
3a	11.43 ± 1.02
3b	35.72 ± 1.57
3c	86.44 ± 1.67
3d	57.09 ± 1.49
3e	17.05 ± 0.83
3f	9.02 ± 0.37
3g	10.74 ± 0.48
3h	10.09 ± 0.42
3i	4.37 ± 0.20
3j	21.16 ± 0.51
3k	6.19 ± 0.27
3l	2.19 ± 0.12
3m	2.88 ± 0.18
3n	3.51 ± 0.16
4	31.78 ± 1.27
STU	4.19 ± 0.17

2.2.2. In Vitro VEGFR-2 Inhibition Assay

VEGFR-2 plays a pivotal role in promoting cancer angiogenesis [35]. VEGFR-2 blockade can exert a direct anticancer impact against cancerous cell lines that express VEGFR-2 receptors on their surface [36]. To elucidate the growth inhibition activity declared by the synthesized hydrazone molecules, VEGFR-2 was evaluated in MCF-7 cells after treatment with 5 μM of the most potent cytotoxic 4-hydroxy-3-methoxybenzylidene hydrazinyl molecule **3l** using ELISA analysis. Sorafenib was used as a positive control in the current study. The inhibitory activity in this assay is given as the percentage inhibition. The obtained results showed good VEGFR-2 inhibition elicited by 4-hydroxy-3-methoxybenzylidene hydrazinyl molecule **3l** compared with Sorafenib (Figure 3). 4-Hydroxy-3-methoxybenzylidene hydrazinyl molecule **3l** showed 80.06% inhibition compared with 88.69% VEGFR-2 inhibition for Sorafenib. Such results concluded that 4-hydroxy-3-methoxybenzylidene hydrazinyl derivative **3l** exerted its anti-proliferative activity through inhibition of VEGFR-2.
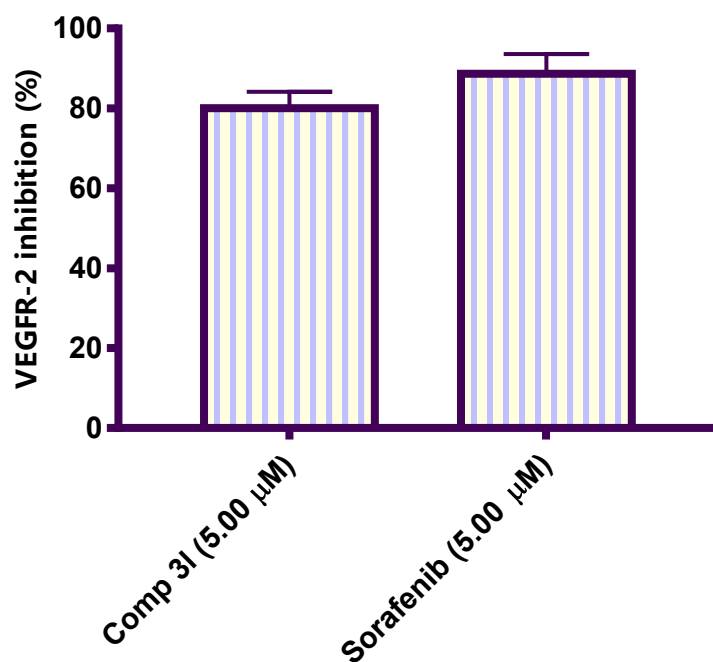
Figure 3. Graphical representation of the in vitro VEGFR-2 kinase inhibition activity (%) in MCF-7 cells treated with 4-hydroxy-3-methoxybenzylidene hydrazinyl molecule **3l** and Sorafenib at 5 μM.

2.2.3. Cell Cycle Analysis

The most active hydrazinyl molecule, **3l**, was selected to be further investigated regarding its impact on cellular cycle progression in the MCF-7 cell line. Exposure of MCF-7 cells to 4-hydroxy-3-methoxybenzylidene hydrazinyl **3l** at a concentration equal to its IC_{50} value (IC_{50} = 2.19 μM) for 48 and its impact on cell cycle stages were analyzed. The results demonstrated that exposure of MCF-7 cells to 4-hydroxy-3-methoxybenzylidene hydrazinyl **3l** resulted in interference with the normal cellular distribution of the tested cell line. In addition, 4-Hydroxy-3-methoxybenzylidene hydrazinyl **3l** induced a significant increase in the percentage of cells at the G1 phase. It is worth mentioning that the percentage of cells accumulated at the G1 phase induced by 4-hydroxy-3-methoxybenzylidene hydrazinyl **3l** was increased by 1.3-fold compared with untreated MCF-7 cells (Figure 4). The results suggested that cellular cycle arrest at the G1 phase might explain the VEGFR-2 inhibitory activity exhibited by 4-hydroxy-3-methoxybenzylidene hydrazinyl **3l**.
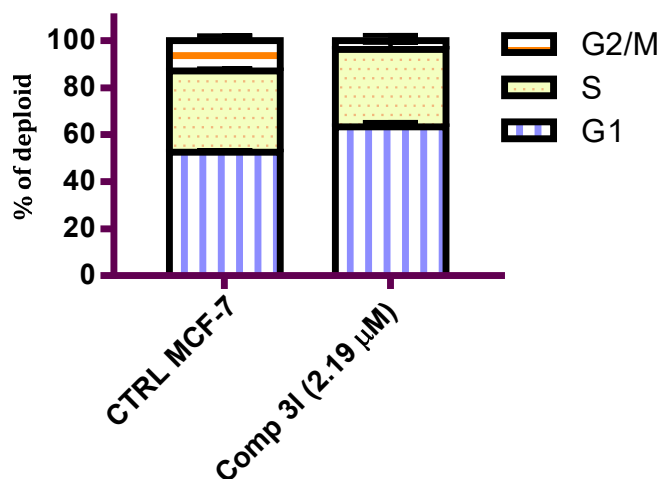

Figure 4. Graphical representation of the effect of 4-hydroxy-3-methoxybenzylidene hydrazinyl **3l** on DNA ploidy flow cytometric analysis of MCF-7 cancer cells after 48 h.

2.2.4. Apoptosis Staining Assay

Modulation of apoptosis provides a protective mechanism against breast carcinoma [37]. To ensure the ability of the synthesized 4-hydroxy-3-methoxybenzylidene hydrazinyl molecule **3l** to induce apoptosis in MCF-7 cells, an apoptosis staining assay was carried out using FACS analysis. Apoptosis staining assay is used to differentiate between live cells, early apoptotic cells, late apoptotic cells, and necrotic cells. After 48 h of treatment with 4-hydroxy-3-methoxybenzylidene hydrazinyl **3l** at a concentration equal to its IC_{50} values (IC_{50} = 2.19 µM), an increase in the percentage of early apoptotic cells (61.6-fold more than control untreated cells). In addition, some treated MCF-7 cells were in a late apoptotic stage (54.2-fold more than control untreated cells) (Figure 5). It can be concluded that the increased percentage of both early and late apoptosis induced by treatment with 4-hydroxy-3-methoxybenzylidene hydrazinyl **3l** provides indirect evidence that this hydrazinyl molecule can arrest cell growth or stimulate apoptosis.
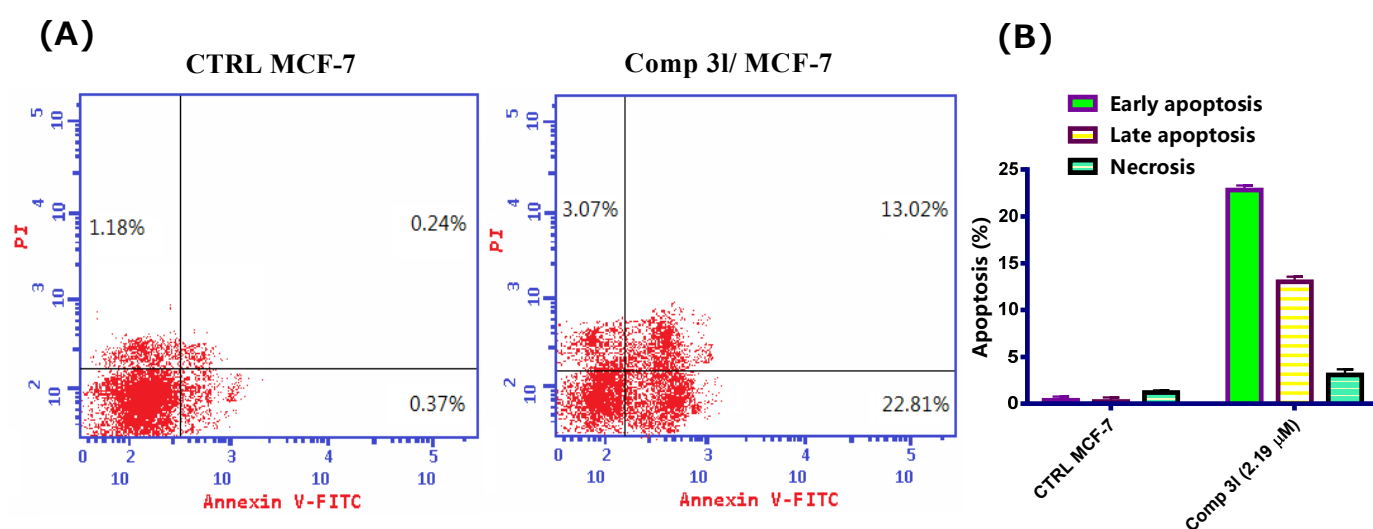

Figure 5. (**A**) Graphical representation of the early and late apoptotic cells percentage after treatment with 4-hydroxy-3-methoxybenzylidene hydrazinyl **3l** compared with untreated MCF-7 cells. (**B**) Representative dot plots of the early and late apoptotic cells percentage of MCF-7 cells treated with 4-hydroxy-3-methoxybenzylidene hydrazinyl **3l** and analyzed by FACS analysis after staining with Annexin V/FITC and PI for 48 h.

2.2.5. Caspase 9 Assay

Apoptosis is well mediated by a subfamily of cysteine proteases known as *c*aspases [38]. *C*aspase 9 is an initiator *c*aspase known to play a major role in mediating mitochondria-induced apoptotic pathways [39]. In the present assay, the level of active *c*aspase 9 was determined in MCF-7 breast cancer cells. As shown in Figure 6, treatment of MCF-7 cells with 4-hydroxy-3-methoxybenzylidene hydrazinyl molecule **3l** at a concentration equal to its IC_{50} value (IC_{50} = 2.19 µM) for 48 h produced a significant increase in the level of active *c*aspase 9 relative to control untreated MCF-7 cells. It is worth mentioning that hydrazinyl molecule **3l** was 8.38-fold more than control untreated cells. Such results suggested that 4-hydroxy-3-methoxybenzylidene hydrazinyl **3l** induced mitochondrial apoptotic pathway.
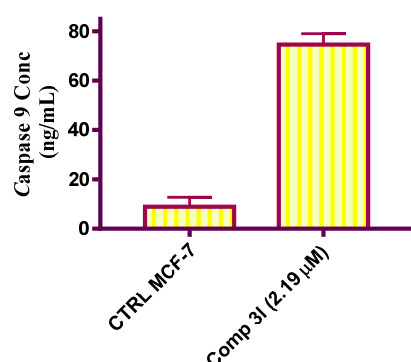
Figure 6. ELISA analysis of active *c*aspase 9 in MCF-7 cells treated with 4-hydroxy-3-methoxybenzylidene hydrazinyl **3l** at its IC_{50} concentration (μM) after 48 h.

3. Conclusions

In conclusion, a series of novel hydrazone derivatives bearing *cis*-(4-chlorostyryl) amide moiety were synthesized and characterized by ^{1}H-NMR, ^{13}C-NMR, and elemental analysis data. They were screened for their cytotoxic activity against the MCF-7 breast cancer cell line. Hydrazinyl molecules **3i**, **3l**, **3m,** and **3n** exhibited potent cytotoxic activity against the test cell line with IC_{50} values of 4.37, 2.19, 2.88, and 3.51 μM, subsequently as compared with STU as reference compound (IC_{50} = 4.19 μM). The cytotoxic activity of the most potent cytotoxic hydrazinyl molecule **3l** appeared to correlate well with its ability to inhibit the VEGFR-2 enzyme. Hydrazinyl molecule **3l** showed 80.06% inhibition against VEGFR-2 at 5 μM compared with Sorafenib (88.69% inhibition at 5 μM). Moreover, activation of the death response pathway induced by hydrazinyl compound **3l** leads to cell cycle arrest at the G1 phase (1.3-fold more than untreated control), and fluorochrome Annexin V/FITC staining assay declared cellular death response proceed through the apoptotic mechanistic pathway. Compound **3l** showed a significant increase in the level of active *c*aspase 9. It is worth mentioning that the level of active *c*aspase 9 was increased by 8.38-fold compared with control untreated MCF-7 cells. The molecules reported in this study represent important candidates that could help to develop more effective antiproliferative agents against breast cancer.

4. Experimental

4.1. Chemistry

Melting points, ^{1}H-NMR, ^{13}C-NMR, as well as elemental microanalyses were performed to elucidate the chemical structure of the prepared hydrazone molecules. See Section 4.1.1 in supplementary data.

4.1.1. General Procedure for the Synthesis of N-((Z)-3-((E)-2-Arylidenehydrazinyl)-1-(4-chlorophenyl)-3-oxoprop-1-en-2-yl)-3,4-dimethoxybenzamides **3a–n**

A mixture of the hydrazinyl derivative **2** (375 mg, 1 mmol) and the respective aromatic aldehyde (1 mmol) in pure ethanol (20 mL) and a few drops of glacial acetic acid (10 drops) was heated to reflux for 5–6 h. After completion of the reaction, the reaction mixture was cooled. After cooling, the separated solid residue was filtered, dried, and crystallized from ethanol (70%) to give the title compound **3a–n**.

N-(*(Z)*-3-((*E*)-2-Benzylidenehydrazinyl)-1-(4-chlorophenyl)-3-oxoprop-1-en-2-yl)-3,4-dimethoxybenzamide (**3a**)

White powder (353 mg, 76%), m.p. 248–250 °C. ^{1}H-NMR (400 MHz, DMSO-d_6, δ ppm): 3.83 (s, 3H, OCH$_3$), 3.85 (s, 3H, OCH$_3$), 7.07 (s, 1H, olefinic CH), 7.10 (d, *J* = 8.5 Hz, 1H, arom.CH), 7.43–7.47 (m, 3H, arom.CH), 7.48 (s, 2H, arom.CH), 7.61 (s, 1H, arom.CH), 7.63 (s, 1H, arom.CH), 7.67 (d, *J* = 11.4 Hz, 2H, arom.CH), 7.72 (d, *J* = 6.5 Hz, 2H, arom.CH), 8.42 (s, 1H, CH=N), 10.00 (s, 1H, NH), 11.76 (s, 1H, NH). ^{13}C-NMR (100 MHz, DMSO-d_6, δ ppm): 56.09 (OCH$_3$), 56.17 (OCH$_3$), 111.45 (C-aromatic), 111.65 (C-aromatic), 121.95

(C-olefinic), 125.91 (C-aromatic), 126.78 (C-olefinic), 127.46 (C-aromatic), 129.07 (C-aromatic), 129.31 (C-aromatic), 130.45 (C-aromatic), 131.31 (C-aromatic), 131.57 (C-aromatic), 133.46 (C-aromatic), 133.71 (C-aromatic), 134.90 (C-aromatic), 147.81 (C=N), 148.76 (C-O), 152.35 (C-O), 162.75 (C=O), 165.87 (C=O). Anal. Calcd. for $C_{25}H_{22}ClN_3O_4$ (463.91): C, 64.72; H, 4.78; N, 9.06. Found: C, 64.61; H, 4.04; N, 7.97.

N-((*Z*)-3-((*E*)-2-(4-Chlorobenzylidene)hydrazinyl)-1-(4-chlorophenyl)-3-oxoprop-1-en-2-yl)-3,4-dimethoxybenzamide (**3b**)

White powder (344 mg, 69%), m.p. 241–243 °C. ^{1}H-NMR (400 MHz, DMSO-d_6, δ ppm): 3.83 (s, 3H, OCH$_3$), 3.85 (s, 3H, OCH$_3$), 7.07 (s, 1H, olefinic CH), 7.10 (d, *J* = 8.5 Hz, 1H, arom.CH), 7.47 (d, *J* = 8.6 Hz, 2H, arom.CH), 7.53 (d, *J* = 8.3 Hz, 2H, arom.CH), 7.60 (s, 1H, arom.CH), 7.64 (d, *J* = 8.7 Hz, 3H, arom.CH), 7.74 (d, *J* = 8.4 Hz, 2H, arom.CH), 8.41 (s, 1H, CH=N), 10.02 (s, 1H, NH), 11.83 (s, 1H, NH). ^{13}C-NMR (100 MHz, DMSO-d_6, δ ppm): 56.09 (OCH$_3$), 56.17 (OCH$_3$), 111.45 (C-aromatic), 111.65 (C-aromatic), 121.95 (C-olefinic), 125.88 (C-aromatic), 126.86 (C-olefinic), 129.08 (C-aromatic), 129.41 (C-aromatic), 131.26 (C-aromatic), 131.38 (C-aromatic), 131.58 (C-aromatic), 133.49 (C-aromatic), 133.68 (C-aromatic), 133.86 (C-aromatic), 134.87 (C-aromatic), 146.45 (C=N), 148.76 (C-O), 152.35 (C-O), 162.82 (C=O), 165.88 (C=O). Anal. Calcd. for $C_{25}H_{21}Cl_2N_3O_4$ (498.36): C, 60.25; H, 4.25; N, 8.43. Found: C, 60.17; H, 4.32; N, 8.53.

N-((*Z*)-1-(4-Chlorophenyl)-3-((*E*)-2-(2-nitrobenzylidene)hydrazinyl)-3-oxoprop-1-en-2-yl)-3,4-dimethoxybenzamide (**3c**)

Pale yellow powder (326 mg, 64%), m.p. 235–237 °C. ^{1}H-NMR (400 MHz, DMSO-d_6, δ ppm): 3.83 (s, 3H, OCH$_3$), 3.85 (s, 3H, OCH$_3$), 7.10 (d, *J* = 7.7 Hz, 2H, olefinic and arom.CH), 7.48 (d, *J* = 8.6 Hz, 2H, arom.CH), 7.60 (s, 1H, arom.CH), 7.73–7.63 (m, 4H, arom.CH), 7.83 (t, *J* = 7.5 Hz, 1H, arom.CH), 8.12 (td, *J* = 15.1, 14.4, 7.6 Hz, 2H, arom.CH), 8.82 (s, 1H, CH=N), 10.04 (s, 1H, NH), 12.12 (s, 1H, NH). ^{13}C-NMR (100 MHz, DMSO-d_6, δ ppm): 56.09 (OCH$_3$), 56.17 (OCH$_3$), 111.47 (C-aromatic), 111.63 (C-aromatic), 121.95 (C-olefinic), 124.78 (C-aromatic), 125.11 (C-aromatic), 125.82 (C-olefinic), 128.34 (C-aromatic), 129.09 (C-aromatic), 129.30 (C-aromatic), 131.06 (C-aromatic), 131.62 (C-aromatic), 133.61 (C-aromatic), 134.19 (C-aromatic), 134.64 (C-aromatic), 134.72 (C-aromatic), 142.80 (C=N), 148.69 (C-NO$_2$), 148.79 (C-O), 152.38 (C-O), 163.03 (C=O), 165.90 (C=O). Anal. Calcd. for $C_{25}H_{21}ClN_4O_6$ (508.91): C, 59.00; H, 4.16; N, 11.01. Found: C, 59.09; H, 4.06; N, 10.88.

N-((*Z*)-1-(4-Chlorophenyl)-3-((*E*)-2-(4-nitrobenzylidene)hydrazinyl)-3-oxoprop-1-en-2-yl)-3,4-dimethoxybenzamide (**3d**)

Pale yellow powder (377 mg, 74%), m.p. 243–245 °C. ^{1}H-NMR (400 MHz, DMSO-d_6, δ ppm): 3.83 (s, 3H, OCH$_3$), 3.85 (s, 3H, OCH$_3$), 7.10 (d, *J* = 9.1 Hz, 2H, olefinic and arom.CH), 7.49 (d, *J* = 8.5 Hz, 2H, arom.CH), 7.60 (s, 1H, arom.CH), 7.67 (t, *J* = 7.5 Hz, 3H, arom.CH), 7.98 (d, *J* = 8.0 Hz, 2H, arom.CH), 8.31 (d, *J* = 8.2 Hz, 2H, arom.CH), 8.52 (s, 1H, CH=N), 10.07 (s, 1H, NH), 12.08 (s, 1H, NH). ^{13}C-NMR (100 MHz, DMSO-d_6, δ ppm): 56.09 (OCH$_3$), 56.17 (OCH$_3$), 111.46 (C-aromatic), 111.64 (C-aromatic), 121.97 (C-olefinic), 124.56 (C-aromatic), 124.75 (C-aromatic), 125.79 (C-olefinic), 127.07 (C-aromatic), 127.14 (C-aromatic), 128.36 (C-aromatic), 129.11 (C-aromatic), 131.11 (C-aromatic), 131.63 (C-aromatic), 133.58 (C-aromatic), 141.23 (C-NO$_2$), 145.24 (C=N), 148.78 (C-O), 152.39 (C-O), 163.07 (C=O), 165.91 (C=O). Anal. Calcd. for $C_{25}H_{21}ClN_4O_6$ (508.91): C, 59.00; H, 4.16; N, 11.01. Found: C, 59.12; H, 4.23; N, 10.91.

N-((*Z*)-1-(4-Chlorophenyl)-3-((*E*)-2-(2-hydroxybenzylidene)hydrazinyl)-3-oxoprop-1-en-2-yl)-3,4-dimethoxybenzamide (**3e**)

White powder (312 mg, 65%), m.p. 242–244 °C. ^{1}H-NMR (400 MHz, DMSO-d_6, δ ppm): 3.83 (s, 3H, OCH$_3$), 3.85 (s, 3H, OCH$_3$), 6.92 (d, *J* = 8.5 Hz, 1H, arom.CH), 6.95 (s, 1H, arom.CH), 7.11 (d, *J* = 8.5 Hz, 1H, arom.CH), 7.13 (s, 1H, olefinic CH), 7.27–7.34 (m, 1H, arom.CH), 7.48 (d, *J* = 8.6 Hz, 2H, arom.CH), 7.51 (d, *J* = 7.7 Hz, 1H, arom.CH), 7.61 (s, 1H, arom.CH), 7.65 (d, *J* = 8.6 Hz, 2H, arom.CH), 7.68 (d, *J* = 8.5 Hz, 1H, arom.CH), 8.60 (s, 1H, CH=N), 10.04 (s, 1H, NH), 11.31 (s, 1H, OH), 12.00 (s, 1H, NH). ^{13}C-NMR (100 MHz,

DMSO-d_6, δ ppm): 56.09 (OCH$_3$), 56.18 (OCH$_3$), 111.46 (C-aromatic), 111.67 (C-aromatic), 116.88 (C-aromatic), 119.16 (C-aromatic), 119.80 (C-aromatic), 121.97 (C-olefinic), 125.86 (C-olefinic), 127.34 (C-aromatic), 127.93 (C-aromatic), 129.10 (C-aromatic), 130.00 (C-aromatic), 130.78 (C-aromatic), 131.61 (C-aromatic), 131.76 (C-aromatic), 133.60 (C-aromatic), 148.53 (C=N), 148.78 (C-O), 152.38 (C-O), 157.92 (C-OH), 162.51 (C=O), 165.93 (C=O). Anal. Calcd. for C$_{25}$H$_{22}$ClN$_3$O$_5$ (479.91): C, 62.57; H, 4.62; N, 8.76. Found: C, 62.72; H, 4.55; N, 8.63.

N-((*Z*)-1-(4-Chlorophenyl)-3-((*E*)-2-(4-hydroxybenzylidene)hydrazinyl)-3-oxoprop-1-en-2-yl)-3,4-dimethoxybenzamide (**3f**)

White powder (341 mg, 71%), m.p. 252–254 °C. ^{1}H-NMR (400 MHz, DMSO-d_6, δ ppm): 3.83 (s, 3H, OCH$_3$), 3.85 (s, 3H, OCH$_3$), 6.84 (d, *J* = 8.5 Hz, 2H, arom.CH), 7.05 (s, 1H, olefinic CH), 7.09 (d, *J* = 8.5 Hz, 1H, arom.CH), 7.46 (d, *J* = 8.6 Hz, 2H, arom.CH), 7.54 (d, *J* = 8.5 Hz, 2H, arom.CH), 7.60 (s, 1H, arom.CH), 7.63 (d, *J* = 8.6 Hz, 2H, arom.CH), 7.68 (d, *J* = 2.6 Hz, 1H, arom.CH), 8.30 (s, 1H, CH=N), 9.96 (s, 2H, NH and OH), 11.53 (s, 1H, NH). ^{13}C-NMR (100 MHz, DMSO-d_6, δ ppm): 56.08 (OCH$_3$), 56.16 (OCH$_3$), 111.44 (C-aromatic), 111.66 (C-aromatic), 116.18 (C-aromatic), 121.93 (C-olefinic), 125.87 (C-aromatic), 125.99 (C-aromatic), 126.60 (C-olefinic), 129.03 (C-aromatic), 129.21 (C-aromatic), 130.55 (C-aromatic), 131.53 (C-aromatic), 133.37 (C-aromatic), 133.80 (C-aromatic), 148.17 (C=N), 148.75 (C-O), 152.31 (C-O), 159.83 (C-OH), 162.43 (C=O), 165.82 (C=O). Anal. Calcd. for C$_{25}$H$_{22}$ClN$_3$O$_5$ (479.91): C, 62.57; H, 4.62; N, 8.76. Found: C, 62.70; H, 4.48; N, 8.58.

N-((*Z*)-1-(4-Chlorophenyl)-3-((*E*)-2-(4-methylbenzylidene)hydrazinyl)-3-oxoprop-1-en-2-yl)-3,4-dimethoxybenzamide (**3g**)

White powder (377 mg, 79%), m.p. 213–215 °C. ^{1}H-NMR (400 MHz, DMSO-d_6, δ ppm): 2.35 (s, 3H, CH$_3$), 3.83 (s, 3H, OCH$_3$), 3.85 (s, 3H, OCH$_3$), 7.06 (s, 1H, olefinic CH), 7.10 (d, *J* = 8.5 Hz, 1H, arom.CH), 7.28 (d, *J* = 7.9 Hz, 2H, arom.CH), 7.47 (d, *J* = 8.6 Hz, 2H, arom.CH), 7.60 (s, 2H), 7.62 (d, *J* = 4.8 Hz, 2H, arom.CH), 7.66 (d, *J* = 11.3 Hz, 2H, arom.CH), 8.38 (s, 1H, CH=N), 9.99 (s, 1H, NH), 11.68 (s, 1H, NH). ^{13}C-NMR (100 MHz, DMSO-d_6, δ ppm): 21.50 (CH$_3$), 56.08 (OCH$_3$), 56.17 (OCH$_3$), 111.45 (C-aromatic), 111.65 (C-aromatic), 121.94 (C-olefinic), 125.93 (C-aromatic), 126.68 (C-olefinic), 127.44 (C-aromatic), 129.06 (C-aromatic), 129.92 (C-aromatic), 131.36 (C-aromatic), 131.55 (C-aromatic), 132.19 (C-aromatic), 133.43 (C-aromatic), 133.74 (C-aromatic), 140.27 (C-aromatic), 147.86 (C=N), 148.76 (C-O), 152.33 (C-O), 162.66 (C=O), 165.85 (C=O). Anal. Calcd. for C$_{26}$H$_{24}$ClN$_3$O$_4$ (477.94): C, 65.34; H, 5.06; N, 8.79. Found: C, 65.18; H, 4.93; N, 8.88.

N-((*Z*)-1-(4-Chlorophenyl)-3-((*E*)-2-(4-methoxybenzylidene)hydrazinyl)-3-oxoprop-1-en-2-yl)-3,4-dimethoxybenzamide (**3h**)

White powder (331 mg, 67%), m.p. 219–221 °C. ^{1}H-NMR (400 MHz, DMSO-d_6, δ ppm): 3.81 (s, 3H, OCH$_3$), 3.83 (s, 3H, OCH$_3$), 3.85 (s, 3H, OCH$_3$), 7.04 (s, 1H, olefinic CH), 7.05 (s, 2H, arom.CH), 7.07 (s, 2H, arom.CH), 7.46 (d, *J* = 8.6 Hz, 2H, arom.CH), 7.65 (s, 2H, arom.CH), 7.82 (d, *J* = 8.8 Hz, 3H, arom.CH), 8.35 (s, 1H, CH=N), 9.98 (s, 1H, NH), 11.61 (s, 1H, NH). ^{13}C-NMR (100 MHz, DMSO-d_6, δ ppm): 55.76 (OCH$_3$), 56.08 (OCH$_3$), 56.16 (OCH$_3$), 111.44 (C-aromatic), 111.66 (C-aromatic), 114.82 (C-aromatic), 121.93 (C-olefinic), 125.96 (C-aromatic), 126.62 (C-olefinic), 127.04 (C-aromatic), 127.45 (C-aromatic), 129.05 (C-aromatic), 130.44 (C-aromatic), 131.54 (C-aromatic), 133.40 (C-aromatic), 133.76 (C-aromatic), 147.72 (C=N), 148.76 (C-O), 152.33 (C-O), 162.14 (C-O), 162.55 (C=O), 165.85 (C=O). Anal. Calcd. for C$_{26}$H$_{24}$ClN$_3$O$_5$ (493.94): C, 63.22; H, 4.90; N, 8.51. Found: C, 63.10; H, 5.02; N, 8.69.

N-((*Z*)-1-(4-Chlorophenyl)-3-((*E*)-2-(3,5-dibromo-4-hydroxybenzylidene)hydrazinyl)-3-oxoprop-1-en-2-yl)-3,4-dimethoxybenzamide (**3i**)

Yellow powder (402 mg, 63%), m.p. 246–248 °C. ^{1}H-NMR (400 MHz, DMSO-d_6, δ ppm): 3.83 (s, 3H, OCH$_3$), 3.85 (s, 3H, OCH$_3$), 7.04 (s, 1H, olefinic CH), 7.10 (d, *J* = 8.5 Hz, 1H, arom.CH), 7.47 (d, *J* = 8.4 Hz, 2H, arom.CH), 7.59 (s, 1H, arom.CH), 7.63 (s, 1H, arom.CH), 7.66 (d, *J* = 10.1 Hz, 2H, arom.CH), 7.89 (s, 2H, arom.CH), 8.26 (s, 1H, CH=N), 9.99 (s, 1H, NH), 10.44 (s, 1H, OH), 11.85 (s, 1H, NH). ^{13}C-NMR (100 MHz, DMSO-d_6, δ ppm): 56.08

(OCH$_3$), 56.17 (OCH$_3$), 111.45 (C-aromatic), 111.64 (C-aromatic), 112.69 (C-aromatic), 121.92 (C-olefinic), 125.88 (C-olefinic), 126.71 (C-olefinic), 129.06 (C-aromatic), 129.52 (C-aromatic), 130.99 (C-aromatic), 131.22 (C-aromatic), 131.58 (C-aromatic), 133.46 (C-aromatic), 133.68 (C-aromatic), 148.76 (C=N), 152.34 (C-O), 152.53 (C-O), 157.87 (C-OH), 162.81 (C=O), 165.87 (C=O). Anal. Calcd. for C$_{25}$H$_{20}$Br$_2$ClN$_3$O$_5$ (637.70): C, 47.09; H, 3.16; N, 6.59. Found: C, 46.93; H, 3.24; N, 6.74.

N-((*Z*)-1-(4-Chlorophenyl)-3-((*E*)-2-(4-(dimethylamino)benzylidene)hydrazinyl)-3-oxoprop-1-en-2-yl)-3,4-dimethoxybenzamide (**3j**)

Dark yellow powder (335 mg, 66%), m.p. 249–251 °C. ^{1}H-NMR (400 MHz, DMSO-d_6, δ ppm): 2.98 (s, 6H, 2CH$_3$), 3.83 (s, 3H, OCH$_3$), 3.85 (s, 3H, OCH$_3$), 6.76 (d, *J* = 8.6 Hz, 2H, arom.CH), 7.05 (s, 1H, olefinic CH), 7.10 (d, *J* = 8.5 Hz, 1H, arom.CH), 7.46 (d, *J* = 8.4 Hz, 2H, arom.CH), 7.52 (d, *J* = 8.6 Hz, 2H, arom.CH), 7.61 (d, *J* = 5.6 Hz, 2H, arom.CH), 7.64 (s, 1H, arom.CH), 7.67 (d, *J* = 8.6 Hz, 1H, arom.CH), 8.27 (s, 1H, CH=N), 9.96 (s, 1H, NH), 11.44 (s, 1H, NH). ^{13}C-NMR (100 MHz, DMSO-d_6, δ ppm): 40.42 (2CH$_3$), 56.08 (OCH$_3$), 56.17 (OCH$_3$), 111.44 (C-aromatic), 111.67 (C-aromatic), 112.30 (C-aromatic), 121.92 (C-olefinic), 122.19 (C-aromatic), 126.04 (C-aromatic), 126.44 (C-olefinic), 128.79 (C-aromatic), 129.02 (C-aromatic), 131.51 (C-aromatic), 131.55 (C-aromatic), 133.32 (C-aromatic), 133.85 (C-aromatic), 148.69 (C=N), 148.75 (C-N), 151.94 (C-O), 152.30 (C-O), 162.24 (C=O), 165.81 (C=O). Anal. Calcd. for C$_{27}$H$_{27}$ClN$_4$O$_4$ (506.98): C, 63.96; H, 5.37; N, 11.05. Found: C, 64.08; H, 5.44; N, 10.96.

N-((*Z*)-1-(4-Chlorophenyl)-3-((*E*)-2-(2-hydroxy-3-methoxybenzylidene)hydrazinyl)-3-oxoprop-1-en-2-yl)-3,4-dimethoxybenzamide (**3k**)

Yellow powder (296 mg, 58%), m.p. 250–252 °C. ^{1}H-NMR (400 MHz, DMSO-d_6, δ ppm): 3.82 (s, 3H, OCH$_3$), 3.83 (s, 3H, OCH$_3$), 3.85 (s, 3H, OCH$_3$), 6.87 (t, *J* = 7.8 Hz, 1H, arom.CH), 7.04 (d, *J* = 7.7 Hz, 1H, arom.CH), 7.11 (dd, *J* = 9.3, 4.6 Hz, 3H, olefinic and arom.CH), 7.48 (d, *J* = 8.4 Hz, 2H, arom.CH), 7.61 (s, 1H, arom.CH), 7.62–7.72 (m, 3H, arom.CH), 8.61 (s, 1H, CH=N), 10.03 (s, 1H, NH), 11.02 (s, 1H, OH), 11.97 (s, 1H, NH). ^{13}C-NMR (100 MHz, DMSO-d_6, δ ppm): 56.09 (OCH$_3$), 56.17 (OCH$_3$), 56.27 (OCH$_3$), 111.46 (C-aromatic), 111.67 (C-aromatic), 114.24 (C-aromatic), 119.39 (C-aromatic), 119.47 (C-aromatic), 121.33 (C-olefinic), 121.96 (C-aromatic), 125.86 (C-olefinic), 127.32 (C-aromatic), 128.35 (C-aromatic), 129.10 (C-aromatic), 130.80 (C-aromatic), 131.60 (C-aromatic), 133.61 (C-aromatic), 147.63 (C=N), 148.39 (C-O), 148.42 (C-OH), 148.78 (C-O), 152.38 (C-O), 162.47 (C=O), 165.92 (C=O). Anal. Calcd. for C$_{26}$H$_{24}$ClN$_3$O$_6$ (509.94): C, 61.24; H, 4.74; N, 8.24. Found: C, 61.35; H, 4.70; N, 8.13.

N-((*Z*)-1-(4-Chlorophenyl)-3-((*E*)-2-(4-hydroxy-3-methoxybenzylidene)hydrazinyl)-3-oxoprop-1-en-2-yl)-3,4-dimethoxybenzamide (**3l**)

White powder (311 mg, 61%), m.p. 226–228 °C. ^{1}H-NMR (400 MHz, DMSO-d_6, δ ppm): 3.81 (s, 3H, OCH$_3$), 3.83 (s, 3H, OCH$_3$), 3.85 (s, 3H, OCH$_3$), 6.98 (d, *J* = 8.4 Hz, 1H, arom.CH), 7.00–7.04 (m, 1H, arom.CH), 7.05 (s, 1H, olefinic.CH), 7.10 (d, *J* = 8.5 Hz, 1H, arom.CH), 7.26 (s, 1H, arom.CH), 7.46 (d, *J* = 8.6 Hz, 2H, arom.CH), 7.60 (s, 1H, arom.CH), 7.62 (s, 1H, arom.CH), 7.63–7.70 (m, 2H), 8.26 (s, 1H, CH=N), 9.31 (s, 1H, OH), 9.97 (s, 1H, NH), 11.56 (s, 1H, NH). ^{13}C-NMR (100 MHz, DMSO-d_6, δ ppm): 56.04 (OCH$_3$), 56.09 (OCH$_3$), 56.17 (OCH$_3$), 111.44 (C-aromatic), 111.66 (C-aromatic), 112.35 (C-aromatic), 112.69 (C-aromatic), 120.63 (C-aromatic), 121.93 (C-olefinic), 125.97 (C-aromatic), 126.63 (C-olefinic), 127.74 (C-aromatic), 129.04 (C-aromatic), 131.40 (C-aromatic), 131.53 (C-aromatic), 133.39 (C-aromatic), 133.78 (C-aromatic), 147.34 (C=N), 148.05 (C-O), 148.75 (C-OH), 150.19 (C-O), 152.32 (C-O), 162.47 (C=O), 165.83 (C=O). Anal. Calcd. for C$_{26}$H$_{24}$ClN$_3$O$_6$ (509.94): C, 61.24; H, 4.74; N, 8.24. Found: C, 61.11; H, 4.84; N, 8.32.

N-((*Z*)-1-(4-Chlorophenyl)-3-((*E*)-2-(3,5-dimethoxybenzylidene)hydrazinyl)-3-oxoprop-1-en-2-yl)-3,4-dimethoxybenzamide (**3m**)

White powder (382 mg, 73%), m.p. 200–202 °C. ^{1}H-NMR (400 MHz, DMSO-d_6, δ ppm): 3.80 (s, 6H, 2OCH$_3$), 3.83 (s, 3H, OCH$_3$), 3.85 (s, 3H, OCH$_3$), 6.58 (s, 1H, arom.CH), 6.86

(d, *J* = 1.8 Hz, 2H, arom.CH), 7.04 (s, 1H, olefinic CH), 7.10 (d, *J* = 8.5 Hz, 1H, arom.CH), 7.47 (d, *J* = 8.6 Hz, 2H, arom.CH), 7.60 (s, 1H, arom.CH), 7.63 (s, 1H, arom.CH), 7.67 (d, *J* = 9.0 Hz, 2H, arom.CH), 8.34 (s, 1H, CH=N), 10.02 (s, 1H, NH), 11.78 (s, 1H, NH). ^{13}C-NMR (100 MHz, DMSO-d_6, δ ppm): 55.80 (OCH$_3$), 56.08 (OCH$_3$), 56.17 (OCH$_3$), 56.49 (OCH$_3$), 102.68 (C-aromatic), 105.22 (C-aromatic), 111.45 (C-aromatic), 111.65 (C-aromatic), 121.93 (C-olefinic), 125.90 (C-aromatic), 126.68 (C-olefinic), 129.07 (C-aromatic), 131.33 (C-aromatic), 131.58 (C-aromatic), 133.46 (C-aromatic), 133.69 (C-aromatic), 136.93 (C-aromatic), 147.72 (C=N), 148.76 (C-O), 152.35 (C-O), 161.15 (2C-O), 162.80 (C=O), 165.89 (C=O). Anal. Calcd. for C$_{27}$H$_{26}$ClN$_3$O$_6$ (523.96): C, 61.89; H, 5.00; N, 8.02. Found: C, 62.03; H, 5.09; N, 7.92.

N-((*Z*)-1-(4-Chlorophenyl)-3-oxo-3-((*E*)-2-(3,4,5-trimethoxybenzylidene)hydrazinyl)prop-1-en-2-yl)-3,4-dimethoxybenzamide (**3n**)

White powder (371 mg, 67%), m.p. 197–199 °C. ^{1}H-NMR (400 MHz, DMSO-d_6, δ ppm): 3.72 (s, 3H, OCH$_3$), 3.83 (s, 3H, OCH$_3$), 3.84 (s, 9H, 3OCH$_3$), 7.01 (s, 2H, arom.CH), 7.03 (s, 1H, olefinic CH), 7.10 (d, *J* = 8.4 Hz, 1H, arom.CH), 7.47 (d, *J* = 8.5 Hz, 2H, arom.CH), 7.60 (s, 1H, arom.CH), 7.63 (s, 1H, arom.CH), 7.67 (d, *J* = 9.1 Hz, 2H, arom.CH), 8.34 (s, 1H, CH=N), 10.02 (s, 1H, NH), 11.76 (s, 1H, NH). ^{13}C-NMR (100 MHz, DMSO-d_6, δ ppm): 56.08 (OCH$_3$), 56.17 (OCH$_3$), 56.41 (2OCH$_3$), 60.58 (OCH$_3$), 104.68 (C-aromatic), 111.45 (C-aromatic), 111.64 (C-aromatic), 121.94 (C-olefinic), 125.90 (C-aromatic), 126.55 (C-olefinic), 129.07 (C-aromatic), 130.40 (C-aromatic), 131.41 (C-aromatic), 131.57 (C-aromatic), 133.44 (C-aromatic), 133.70 (C-aromatic), 139.61 (C-O), 147.86 (C=N), 148.76 (C-O), 152.35 (C-O), 153.66 (2C-O), 162.73 (C=O), 165.91 (C=O). Anal. Calcd. for C$_{28}$H$_{28}$ClN$_3$O$_7$ (553.99): C, 60.70; H, 5.09; N, 7.58. Found: C, 60.84; H, 4.98; N, 7.47.

4.1.2. General Procedure for the Synthesis of *N*-((*Z*)-1-(4-Chlorophenyl)-3-oxo-3-((*E*)-2-((*E*)-3-phenylallylidene)hydrazinyl)prop-1-en-2-yl)-3,4-dimethoxybenzamide (**4**)

A mixture of the hydrazinyl derivative **2** (375 mg, 1 mmol) and cinnamaldehyde (132 mg, 1 mmol) in glacial acetic acid (20 mL) was heated to reflux for 4 h. After completion of the reaction, the reaction mixture was cooled. After cooling, the reaction mixture was poured into ice-cold water, and the separated solid was filtered, dried, and crystallized from ethanol (70%) to afford pure compound **4**.

White powder (402 mg, 82%), m.p. 226–228 °C. ^{1}H-NMR (400 MHz, DMSO-d_6, δ ppm): 3.83 (s, 3H, OCH$_3$), 3.85 (s, 3H, OCH$_3$), 7.05 (d, *J* = 7.4 Hz, 3H, olefinic and arom.CH), 7.10 (d, *J* = 8.5 Hz, 1H, olefinic CH), 7.34 (d, *J* = 7.2 Hz, 1H, olefinic CH), 7.40 (t, *J* = 7.4 Hz, 2H, arom.CH), 7.46 (d, *J* = 8.6 Hz, 2H, arom.CH), 7.61 (d, *J* = 8.5 Hz, 3H, arom.CH), 7.63–7.74 (m, 3H, arom.CH), 8.20 (d, *J* = 7.5 Hz, 1H, CH=N), 9.97 (s, 1H, NH), 11.65 (s, 1H, NH). ^{13}C-NMR (100 MHz, DMSO-d_6, δ ppm): 56.09 (OCH$_3$), 56.17 (OCH$_3$), 111.45 (C-aromatic), 111.66 (C-aromatic), 121.95 (C-olefinic), 125.94 (C-aromatic), 126.21 (C-olefinic), 126.85 (C-olefinic), 127.54 (C-aromatic), 129.05 (C-aromatic), 129.29 (C-aromatic), 131.26 (C-aromatic), 131.55 (C-aromatic), 133.44 (C-aromatic), 133.75 (C-aromatic), 136.41 (C-olefinic), 139.23 (C-aromatic), 148.76 (C=N), 149.91 (C-O), 152.34 (C-O), 162.60 (C=O), 165.83 (C=O). Anal. Calcd. for C$_{27}$H$_{24}$ClN$_3$O$_4$ (489.95): C, 66.19; H, 4.94; N, 8.58. Found: C, 66.27; H, 5.02; N, 8.46.

4.2. Biological Study

4.2.1. MTT Assay against MCF-7 Breast Cancer Cell Line

MTT assay was carried out to investigate the cytotoxic effect of the newly synthesized hydrazone molecules **3a–n** and **4** on the breast adenocarcinoma (MCF-7) cell line. See Section 4.2.1 in the supplementary material.

4.2.2. VEGFR-2 Inhibition Assay

VEGFR-2 inhibition assay was performed utilizing ELISA analysis for 4-hydroxy-3-methoxybenzylidene hydrazinyl molecule **3l** compared with Sorafenib. See Section 4.2.2 in the supplementary material.

4.2.3. Cell Cycle Analysis

Cell cycle analysis in MCF-7 cells for 4-hydroxy-3-methoxybenzylidene hydrazinyl molecule **3l** by FACS analysis was performed. See Section 4.2.3 in the supplementary material.

4.2.4. Annexin V/FITC Staining Assay

Annexin V-FITC/PI double staining assay in MCF-7 cells for 4-hydroxy-3-methoxybenzylidene hydrazinyl molecule **3l** by FACS analysis was performed according to the manufacturer's directions. See Section 4.2.4 in the supplementary material.

4.2.5. *Caspase 9 Assay*

Caspase 9 was measured for 4-hydroxy-3-methoxybenzylidene hydrazinyl molecule **3l** by ELISA analysis in MCF-7 cells according to the manufacturer's directions. See Section 4.2.5 in the supplementary material.

Supplementary Materials: The following supporting information can be downloaded at: https://www.mdpi.com/article/10.3390/sym14112457/s1, Figure S1: ^{1}H-NMR spectrum of compound **3a**, Figure S2: ^{13}C-NMR spectrum of compound **3a**, Figure S3: ^{1}H-NMR spectrum of compound **3b**, Figure S4: ^{13}C-NMR spectrum of compound **3b**, Figure S5: ^{1}H-NMR spectrum of compound **3c**, Figure S6: ^{13}C-NMR spectrum of compound **3c**, Figure S7: ^{1}H-NMR spectrum of compound **3d**, Figure S8: ^{13}C-NMR spectrum of compound **3d**, Figure S9: ^{1}H-NMR spectrum of compound **3e**, Figure S10: ^{13}C-NMR spectrum of compound **3e**, Figure S11: ^{1}H-NMR spectrum of compound **3f**, Figure S12: ^{13}C-NMR spectrum of compound **3f**, Figure S13: ^{1}H-NMR spectrum of compound **3g**, Figure S14: ^{13}C-NMR spectrum of compound **3g**, Figure S15: ^{1}H-NMR spectrum of compound **3h**, Figure S16: ^{13}C-NMR spectrum of compound **3h**, Figure S17: ^{1}H-NMR spectrum of compound **3i**, Figure S18: ^{13}C-NMR spectrum of compound **3i**, Figure S19: ^{1}H-NMR spectrum of compound **3j**, Figure S20: ^{13}C-NMR spectrum of compound **3j**, Figure S21: ^{1}H-NMR spectrum of compound **3k**, Figure S22: ^{13}C-NMR spectrum of compound **3k**, Figure S23: ^{1}H-NMR spectrum of compound **3l**, Figure S24: ^{13}C-NMR spectrum of compound **3l**, Figure S25: ^{1}H-NMR spectrum of compound **3m**, Figure S26: ^{13}C-NMR spectrum of compound **3m**. Figure S27: ^{1}H-NMR spectrum of compound **3n**, Figure S28: ^{13}C-NMR spectrum of compound **3n**, Figure S29: ^{1}H-NMR spectrum of compound **4**, Figure S30: ^{13}C-NMR spectrum of compound **4**; and detailed descriptions for Sections 4.1.1 and 4.2.1–4.2.5.

Conflicts of Interest: The authors declare no conflict of interest.

References

1. Siegel, R.L.; Miller, K.D.; Fuchs, H.E.; Jemal, A. Cancer statistics, 2021. *CA Cancer J. Clin.* **2021**, *71*, 7–33. [CrossRef] [PubMed]
2. Hulvat, M.C. Cancer incidence and trends. *Surg. Clin.* **2020**, *100*, 469–481. [CrossRef]
3. Tsao, C.W.; Aday, A.W.; Almarzooq, Z.I.; Alonso, A.; Beaton, A.Z.; Bittencourt, M.S.; Boehme, A.K.; Buxton, A.E.; Carson, A.P.; Commodore-Mensah, Y. Heart disease and stroke statistics—2022 update: A report from the American Heart Association. *Circulation* **2022**, *145*, e153–e639. [CrossRef]

4.   Mansoori, B.; Mohammadi, A.; Davudian, S.; Shirjang, S.; Baradaran, B. The different mechanisms of cancer drug resistance: A brief review. *Adv. Pharm. Bull.* **2017**, *7*, 339–348. [CrossRef] [PubMed]

5.   Naing, A.; Hajjar, J.; Gulley, J.L.; Atkins, M.B.; Ciliberto, G.; Meric-Bernstam, F.; Hwu, P. Strategies for improving the management of immune-related adverse events. *J. Immunother. Cancer* **2020**, *8*, e001754. [CrossRef]

6.   Hussain, Y.; Islam, L.; Khan, H.; Filosa, R.; Aschner, M.; Javed, S. Curcumin–cisplatin chemotherapy: A novel strategy in promoting chemotherapy efficacy and reducing side effects. *Phytother. Res.* **2021**, *35*, 6514–6529. [CrossRef] [PubMed]

7.   Huelse, J.M.; Fridlyand, D.M.; Earp, S.; DeRyckere, D.; Graham, D.K. MERTK in cancer therapy: Targeting the receptor tyrosine kinase in tumor cells and the immune system. *Pharmacol.Ther.* **2020**, *213*, 107577. [CrossRef]

8.   Kongkrongtong, T.; Sumigama, Y.; Nagamune, T.; Kawahara, M. Reprogramming signal transduction through a designer receptor tyrosine kinase. *Commun. Biol.* **2021**, *4*, 752. [CrossRef]

9.   Roskoski, R. Small molecule inhibitors targeting the EGFR/ErbB family of protein-tyrosine kinases in human cancers. *Pharmacol. Res.* **2019**, *139*, 395–411. [CrossRef]

10.   Saraon, P.; Pathmanathan, S.; Snider, J.; Lyakisheva, A.; Wong, V.; Stagljar, I. Receptor tyrosine kinases and cancer: Oncogenic mechanisms and therapeutic approaches. *Oncogene* **2021**, *40*, 4079–4093. [CrossRef]

11.   Tripathi, S.K.; Pandey, K.; Rengasamy, K.R.R.; Biswal, B.K. Recent updates on the resistance mechanisms to epidermal growth factor receptor tyrosine kinase inhibitors and resistance reversion strategies in lung cancer. *Med. Res. Rev.* **2020**, *40*, 2132–2176. [CrossRef]

12.   Xu, Y.; Wang, J.; Wang, X.; Zhou, X.; Tang, J.; Jie, X.; Yang, X.; Rao, X.; Xu, Y.; Xing, B.; et al. Targeting ADRB2 enhances sensitivity of non-small cell lung cancer to VEGFR2 tyrosine kinase inhibitors. *Cell Death Discov.* **2022**, *8*, 36. [CrossRef]

13.   Modi, S.J.; Kulkarni, V.M. Vascular Endothelial Growth Factor Receptor (VEGFR-2)/KDR Inhibitors: Medicinal Chemistry Perspective. *Med. Drug Discov.* **2019**, *2*, 100009. [CrossRef]

14.   Wang, X.; Bove, A.M.; Simone, G.; Ma, B. Molecular bases of VEGFR-2-mediated physiological function and pathological role. *Front. Cell Dev. Biol.* **2020**, *8*, 599281. [CrossRef]

15.   Mariotti, V.; Fiorotto, R.; Cadamuro, M.; Fabris, L.; Strazzabosco, M. New insights on the role of vascular endothelial growth factor in biliary pathophysiology. *JHEP Rep.* **2021**, *3*, 100251. [CrossRef]

16.   Farghaly, T.A.; Al-Hasani, W.A.; Abdulwahab, H.G. An updated patent review of VEGFR-2 inhibitors (2017-present). *Expert Opin. Ther. Pat.* **2021**, *31*, 989–1007. [CrossRef] [PubMed]

17.   Al-Salem, H.S.; Arifuzzaman, M.; Issa, I.S.; Rahman, A.F.M.M. Isatin-Hydrazones with Multiple Receptor Tyrosine Kinases (RTKs) Inhibitory Activity and In-Silico Binding Mechanism. *Appl. Sci.* **2021**, *11*, 3746. [CrossRef]

18.   Mali, S.N.; Thorat, B.R.; Gupta, D.R.; Pandey, A. Mini-Review of the Importance of Hydrazides and Their Derivatives—Synthesis and Biological Activity. *Eng. Proc.* **2021**, *11*, 21.

19.   Abdelrhman, E.M.; El-Shetary, B.A.; Shebl, M.; Adly, O.M.I. Coordinating behavior of hydrazone ligand bearing chromone moiety towards Cu(II) ions: Synthesis, spectral, density functional theory (DFT) calculations, antitumor, and docking studies. *Appl. Organomet. Chem.* **2021**, *35*, e6183. [CrossRef]

20.   Guimaraes, D.G.; de Assis Gonsalves, A.; Rolim, L.A.; Araújo, E.C.; dos Anjos, S.; Laysna, V.; Silva, M.F.; de Cássia Evangelista de Oliveira, F.; da Costa, M.P.; Pessoa, C. Naphthoquinone-based hydrazone hybrids: Synthesis and potent activity against cancer cell lines. *Med. Chem.* **2021**, *17*, 945–955. [CrossRef] [PubMed]

21.   de Oliveira Carneiro Brum, J.; França, T.C.; LaPlante, S.R.; Villar, J.D.F. Synthesis and biological activity of hydrazones and derivatives: A review. *Mini Rev. Med. Chem.* **2020**, *20*, 342–368. [CrossRef]

22.   Baldisserotto, A.; Demurtas, M.; Lampronti, I.; Tacchini, M.; Moi, D.; Balboni, G.; Vertuani, S.; Manfredini, S.; Onnis, V. In-Vitro Evaluation of Antioxidant, Antiproliferative and Photo-Protective Activities of Benzimidazolehydrazone Derivatives. *Pharmaceuticals* **2020**, *13*, 68. [CrossRef] [PubMed]

23.   Khattab, T.A. From chromic switchable hydrazones to smart materials. *Mater. Chem. Phys.* **2020**, *254*, 123456. [CrossRef]

24.   Liu, B.; Liu, H.; Zhang, H.; Di, Q.; Zhang, H. Crystal Engineering of a Hydrazone Molecule toward High Elasticity and Bright Luminescence. *J. Phys. Chem. Lett.* **2020**, *11*, 9178–9183. [CrossRef] [PubMed]

25.   Han, M.İ.; Atalay, P.; Tunç, C.Ü.; Ünal, G.; Dayan, S.; Aydın, Ö.; Küçükgüzel, Ş.G. Design and synthesis of novel (S)-Naproxen hydrazide-hydrazones as potent VEGFR-2 inhibitors and their evaluation in vitro/in vivo breast cancer models. *Bioorg. Med. Chem.* **2021**, *37*, 116097. [CrossRef]

26.   Hantgan, R.R.; Stahle, M.C. Integrin Priming Dynamics: Mechanisms of Integrin Antagonist-Promoted αIIbβ3:PAC-1 Molecular Recognition. *Biochemistry* **2009**, *48*, 8355–8365. [CrossRef] [PubMed]

27.   Şenkardeş, S.; İhsan Han, M.; Gürboğa, M.; Özakpinar, Ö.B.; Güniz Küçükgüzel, Ş. Synthesis and anticancer activity of novel hydrazone linkage-based aryl sulfonate derivatives as apoptosis inducers. *Med. Chem. Res.* **2022**, *31*, 368–379. [CrossRef]

28.   El-Adl, K.; Abdel-Rahman, A.A.H.; Omar, A.M.; Alswah, M.; Saleh, N.M. Design, synthesis, anticancer, and docking of some S- and/or N-heterocyclic derivatives as VEGFR-2 inhibitors. *Arch. Pharm.* **2022**, *355*, 2100237. [CrossRef]

29.   Takao, K.; Yahagi, H.; Uesawa, Y.; Sugita, Y. 3-(E)-Styryl-2H-chromene derivatives as potent and selective monoamine oxidase B inhibitors. *Bioorg. Chem.* **2018**, *77*, 436–442. [CrossRef]

30.   Wei, X.-W.; Yuan, J.-M.; Huang, W.-Y.; Chen, N.-Y.; Li, X.-J.; Pan, C.-X.; Mo, D.-L.; Su, G.-F. 2-Styryl-4-aminoquinazoline derivatives as potent DNA-cleavage, p53-activation and in vivo effective anticancer agents. *Eur. J. Med. Chem.* **2020**, *186*, 111851. [CrossRef]

31. Abe, H.; Okazawa, M.; Oyama, T.; Yamazaki, H.; Yoshimori, A.; Kamiya, T.; Tsukimoto, M.; Takao, K.; Sugita, Y.; Sakagami, H.; et al. A Unique Anti-Cancer 3-Styrylchromone Suppresses Inflammatory Response via HMGB1-RAGE Signaling. *Medicines* **2021**, *8*, 17. [CrossRef]

32. Yang, X.; Cheng, B.; Xiao, Y.; Xue, M.; Liu, T.; Cao, H.; Chen, J. Discovery of novel CA-4 analogs as dual inhibitors of tubulin polymerization and PD-1/PD-L1 interaction for cancer treatment. *Eur. J. Med. Chem.* **2021**, *213*, 113058. [CrossRef]

33. Lee, H.-Z.; Kwitkowski, V.E.; Del Valle, P.L.; Ricci, M.S.; Saber, H.; Habtemariam, B.A.; Bullock, J.; Bloomquist, E.; Li Shen, Y.; Chen, X.-H.; et al. FDA Approval: Belinostat for the Treatment of Patients with Relapsed or Refractory Peripheral T-cell Lymphoma. *Clin. Cancer Res.* **2015**, *21*, 2666–2670. [CrossRef] [PubMed]

34. Kassab, A.E.; Gedawy, E.M. Novel ciprofloxacin hybrids using biology oriented drug synthesis (BIODS) approach: Anticancer activity, effects on cell cycle profile, caspase-3 mediated apoptosis, topoisomerase II inhibition, and antibacterial activity. *Eur. J. Med. Chem.* **2018**, *150*, 403–418. [CrossRef]

35. Melincovici, C.S.; Boşca, A.B.; Şuşman, S.; Mărginean, M.; Mihu, C.; Istrate, M.; Moldovan, I.-M.; Roman, A.L.; Mihu, C.M. Vascular endothelial growth factor (VEGF)-key factor in normal and pathological angiogenesis. *Rom. J. Morphol. Embryol.* **2018**, *59*, 455–467.

36. Yang, C.; Qin, S. Apatinib targets both tumor and endothelial cells in hepatocellular carcinoma. *Cancer Med.* **2018**, *7*, 4570–4583. [CrossRef]

37. Owen, H.C.; Appiah, S.; Hasan, N.; Ghali, L.; Elayat, G.; Bell, C. Chapter Eleven - Phytochemical Modulation of Apoptosis and Autophagy: Strategies to Overcome Chemoresistance in Leukemic Stem Cells in the Bone Marrow Microenvironment. *Int. Rev. Neurobiol.* **2017**, *135*, 249–278. [PubMed]

38. Kesavardhana, S.; Malireddi, R.S.; Kanneganti, T.-D. Caspases in cell death, inflammation, and gasdermin-induced pyroptosis. *Annu. Rev. Immunol.* **2020**, *38*, 567–582. [CrossRef]

39. Araya, L.E.; Soni, I.V.; Hardy, J.A.; Julien, O. Deorphanizing Caspase-3 and Caspase-9 Substrates In and Out of Apoptosis with Deep Substrate Profiling. *ACS Chem. Biol.* **2021**, *16*, 2280–2296. [CrossRef] [PubMed]